

The First Bis(μ -oxo)diiron(III) Complex. Structure and Magnetic Properties of $[\text{Fe}_2(\mu\text{-O})_2(6\text{TLA})_2](\text{ClO}_4)_2$

Yan Zang, Yanhong Dong, and Lawrence Que, Jr.*

Department of Chemistry, University of Minnesota
Minneapolis, Minnesota 55455

Karl Kauffmann and Eckard Münck*

Department of Chemistry, Carnegie-Mellon University
Pittsburgh, Pennsylvania 15213

Received October 17, 1994

The bis(μ -oxo)dimetal core is a common structural motif for higher valent dinuclear manganese complexes^{1,2} and is believed to be present in the active sites of Mn catalase³ and the oxygen-evolving complex of photosynthesis.⁴ Crystallographically characterized examples of such cores for iron are thus far unknown; however, bis(μ -oxo)diiron species have recently been suggested as possible intermediates in the oxygen activation mechanism of methane monooxygenase.^{5,6} Our interest in this subject has led to the isolation of a high-valent intermediate formulated as a bis(μ -oxo)diiron(III,IV) complex on the basis of a number of spectroscopic measurements.⁶ We have also characterized the complex $[\text{Fe}_2(\text{O})(\text{OH})(6\text{TLA})_2](\text{ClO}_4)_3$ (**1**),⁷ the only diiron complex with a (μ -oxo)(μ -hydroxo)diiron(III) core.⁸ Treatment of **1** with 1 equiv of Et_3N affords $[\text{Fe}_2(\text{O})_2(6\text{TLA})_2](\text{ClO}_4)_2$ (**2**),⁹ the first complex with a bis(μ -oxo)diiron(III) core. We describe its structural and magnetic properties here.

The crystal structure of **2**,¹⁰ shown in Figure 1, consists of a centrosymmetric $\text{Fe}_2(\mu\text{-O})_2$ rhomb with the 6TLA nitrogens completing the coordination sphere of each metal center. Compared to diiron(III) complexes with a single oxo bridge,¹¹ **2** exhibits some unique structural features. Firstly, the Fe– μ -O bonds of **2**, namely 1.841(4) Å for the Fe– μ -O bond *trans* to the amine nitrogen and 1.917(4) Å for the Fe– μ -O bond *trans* to one of the pyridines, are significantly longer than those of any (μ -oxo)diiron(III) complex (range 1.73–1.83 Å).¹¹ We attribute the lengthening of the Fe– μ -O bonds to the presence

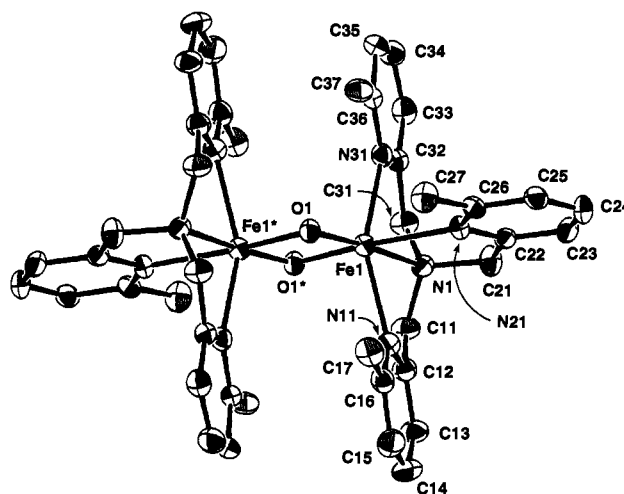


Figure 1. ORTEP drawing of the cation of **2** with atom labeling scheme. Selected bond lengths (Å) and bond angles (deg) are as follows: Fe1–O1, 1.841(4); Fe1–O1', 1.917(4); Fe1–N1, 2.192(5); Fe1–N11, 2.272(5); Fe1–N21, 2.249(4); Fe1–N31, 2.252(5); Fe1–Fe1', 2.714(2); Fe1–O1–Fe1', 92.5(2); N21–Fe1–O1, 166.8(2); N21A–Fe1A–O1A', 105.7(2).

of a second oxo bridge that mitigates the Lewis acidity of the iron center. In agreement with this notion, the Fe– μ -O and average Fe–N bonds of its conjugate acid **1** are shorter than those of **2** (Table 1).⁸ Similarly, the average Mn– μ -O bond found for $[\text{Mn}^{\text{III}}_2(\mu\text{-O})_2]$ complexes (1.84 Å)² is noticeably longer than that found for $[\text{Mn}^{\text{III}}(\mu\text{-O})]$ complexes (av 1.79 Å).¹ Secondly, the Fe–O–Fe angle of 92.5(2)^o is the smallest for (μ -oxo)diiron(III) complexes and may reflect increased repulsion between the two oxo bridges. Thirdly, the oxo bridges of **2** have a significant asymmetry ($\Delta r = 0.076$ Å); this asymmetry may be an intrinsic feature of the Fe_2O_2 rhomb, as suggested from a comparison with $\text{Fe}_2(\mu\text{-OH})_2$ and $\text{Fe}_2(\mu\text{-OR})_2$ complexes, which have comparable Δr values.¹² In contrast, the $[\text{Mn}^{\text{III}}_2(\mu\text{-O})_2]$ complexes do not exhibit such pronounced asymmetry.² Lastly, the Fe–Fe separation decreases from 2.95(1) Å in **1** to 2.714(2) Å in **2**, making the latter the smallest separation observed for a (μ -oxo)diiron(III) unit¹¹ but comparable to those observed for $[\text{Mn}_2(\mu\text{-O})_2]^{n+}$ ($n = 2, 3, 4$) complexes.^{1,2} This shortening of the metal–metal distance upon deprotonation has also been observed for the series $[\text{Mn}_2(\mu\text{-OH})_2(\text{salpn})_2]^{2+}$, $[\text{Mn}_2(\mu\text{-O})(\mu\text{-OH})(\text{salpn})_2]^+$, and $[\text{Mn}_2(\mu\text{-O})_2(\text{salpn})_2]$.¹³

Polycrystalline **2** exhibits a 4.2 K zero field Mössbauer spectrum (Figure 2A) consisting of one sharp doublet with $\Delta E_Q = 1.93$ mm/s and $\delta = 0.50$ mm/s (relative to Fe metal at 298 K). Its 8.0 T spectrum (Figure 2B) exhibits a pattern typical of a diamagnetic complex. These properties (ΔE_Q , δ , $S = 0$ at 4.2 K) are very similar to those observed for the antiferromagnetically coupled diiron(III) sites of iron–oxo proteins and relevant model compounds including **1**.^{5,8,14} However, **1** and **2** differ from other (μ -oxo)diiron complexes in their magnetic properties. The temperature dependence of the magnetic susceptibility of **2**, shown in Figure 3, is best fit with $J = +54$ –(8) cm^{-1} ($\mathbf{H} = J\mathbf{S}_1\mathbf{S}_2$). Independently, we have determined J with Mössbauer spectroscopy,¹⁵ obtaining $J = +68$ (10) cm^{-1} .

(1) Wieghardt, K. *Angew. Chem., Int. Ed. Engl.* **1989**, *28*, 1153–1172.

(2) (a) Goodson, P. A.; Oki, A. R.; Glerup, J.; Hodgson, D. J. *J. Am. Chem. Soc.* **1990**, *112*, 6248–6254. (b) Glerup, J.; Goodson, P. A.; Hazell, A.; Hazell, R.; Hodgson, D. J.; McKenzie, C. J.; Michelsen, K.; Rychlewski, U.; Toftlund, H. *Inorg. Chem.* **1994**, *33*, 4105–4111.

(3) Waldo, G. S.; Yu, S.; Penner-Hahn, J. E. *J. Am. Chem. Soc.* **1992**, *114*, 5869–5870.

(4) (a) Klein, M. P.; Sauer, K.; Yachandra, V. K. *Photosynth. Res.* **1993**, *38*, 265–277. (b) Penner-Hahn, J. E.; Fronko, R. M.; Pecoraro, V. L.; Yocum, C. F.; Betts, S. D.; Bowlby, N. R. *J. Am. Chem. Soc.* **1990**, *112*, 2549–2557.

(5) Feig, A. L.; Lippard, S. J. *Chem. Rev.* **1994**, *94*, 759–805.

(6) Dong, Y.; Fujii, H.; Hendrich, M. P.; Leising, R. A.; Pan, G.; Randall, C. R.; Wilkinson, E. C.; Zang, Y.; Que, L., Jr.; Fox, B. G.; Kauffmann, K.; Münck, E. *J. Am. Chem. Soc.*, submitted.

(7) Abbreviations used: HBPz, hydrotris(pyrazolyl)borate anion; HPTB, N,N,N',N' -tetrakis(2-benzimidazolyl)-1,3-diamino-2-hydroxypropane; salpn, N,N' -(1,3-propane)bis(salicylideneamine); 6TLA, tris(6-methylpyridyl-2-methyl)amine.

(8) Zang, Y.; Pan, G.; Que, L., Jr.; Fox, B. G.; Münck, E. *J. Am. Chem. Soc.* **1994**, *116*, 3653–3654.

(9) Anal. for $2\cdot 2\text{THF}\cdot 2\text{H}_2\text{O}$. Calcd for $\text{C}_{50}\text{H}_{68}\text{Cl}_2\text{Fe}_2\text{N}_8\text{O}_{14}$: C, 50.56; H, 5.73; N, 9.43. Found: C, 50.76; H, 5.60; N, 9.47. UV-vis (CH_3CN): 320 nm ($\epsilon = 4200 \text{ M}^{-1} \text{ cm}^{-1}$), 375 nm (sh, $\epsilon \sim 2000 \text{ M}^{-1} \text{ cm}^{-1}$), 470 nm ($\epsilon = 560 \text{ M}^{-1} \text{ cm}^{-1}$). **Caution!** Metal complexes with organic ligands and perchlorate anions are potentially explosive.

(10) Crystal data for $2\cdot 2\text{THF}$ ($\text{C}_{50}\text{H}_{64}\text{Cl}_2\text{Fe}_2\text{N}_8\text{O}_{12}$, FW 1151.70) at 173 K: dark red wedges, monoclinic, space group $P2_1/n$ (No. 14), $a = 13.222$ –(5) Å, $b = 14.062$ –(7) Å, $c = 14.82$ –(1) Å, $\beta = 112.76$ –(6) $^\circ$, $V = 2540$ –(5) Å³, $Z = 2$. For 3081 unique, observed reflections with $I > 2\sigma(I)$ and 334 parameters, the current discrepancy indices are $R = 0.065$, $R_w = 0.066$.

(11) Kurtz, D. M., Jr. *Chem. Rev.* **1990**, *90*, 585–606.

(12) (a) Thich, J. A.; Ou, C. C.; Powers, D.; Vasiliou, B.; Mastropaolo, D.; Potenza, J. A.; Schugar, H. J. *J. Am. Chem. Soc.* **1976**, *98*, 1425–1433. (b) Borer, L.; Thalken, L.; Ceccarelli, C.; Glick, M.; Zhang, J. H.; Reiff, W. M. *Inorg. Chem.* **1983**, *22*, 1719–1724. (c) Walker, J. D.; Poli, R. *Inorg. Chem.* **1990**, *29*, 756–761. (d) Ménage, S.; Que, L., Jr. *Inorg. Chem.* **1990**, *29*, 4293–4297.

(13) Baldwin, M. J.; Stemmler, T. L.; Riggs-Gelasco, P. J.; Kirk, M. L.; Penner-Hahn, J. E.; Pecoraro, V. L. *J. Am. Chem. Soc.* **1994**, *116*, 11349–11356.

(14) Que, L., Jr.; True, A. E. In *Progress in Inorganic Chemistry*; Lippard, S. J., Ed.; John Wiley & Sons: New York, 1990; Vol. 38; pp 97–200.

Table 1. Comparison of the Properties of **1** and **2**

property	[Fe ₂ (O)(OH)(6TLA) ₂](ClO ₄) ₃ (1)	[Fe ₂ (O) ₂ (6TLA) ₂](ClO ₄) ₂ (2)
$r(\text{Fe}-\mu\text{-O})$, Å	1.82 ^a	1.841(4), 1.917(4)
$r(\text{Fe}-\mu\text{-OH})$, Å	1.99 ^a	
av $r(\text{Fe}-\text{N})$, Å	2.20 ^b	2.24
$r(\text{Fe}-\text{Fe})$	2.95(1) ^b	2.714(2)
$\angle\text{Fe}-\mu\text{-O}-\text{Fe}$ (deg)	106 ^a	92.5(2)
δ (mm/s)	0.51	0.50
ΔE_Q (mm/s)	1.66	1.93
J (cm ⁻¹ , $\mathbf{H} = J\mathbf{S}_1\mathbf{S}_2$)	112	61 ^c

^a Derived from EXAFS data from ref 8. ^b Derived from crystallographic data from ref 8. ^c Average of values from susceptibility and Mössbauer studies.

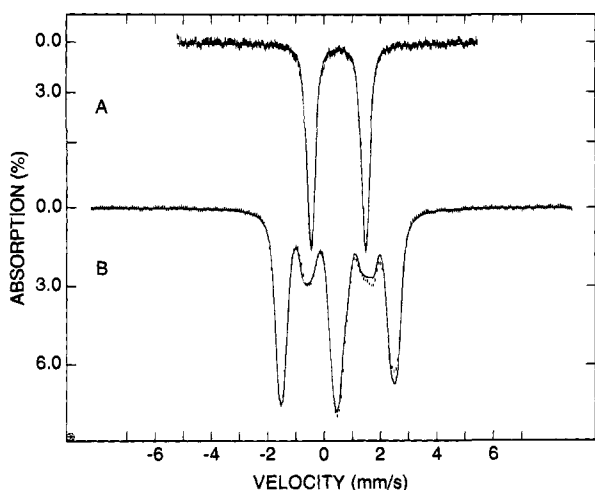


Figure 2. 4.2 K Mössbauer spectra of polycrystalline **1** recorded in zero field (A) and in a parallel applied field of 8.0 T (B). The solid line in (A) is a least-squares fit to one quadrupole doublet. The solid line in (B) is a spectral simulation for $\Delta E_Q = +1.93$ mm/s and $\eta = 0.8$, assuming an isolated ground state with $S = 0$.

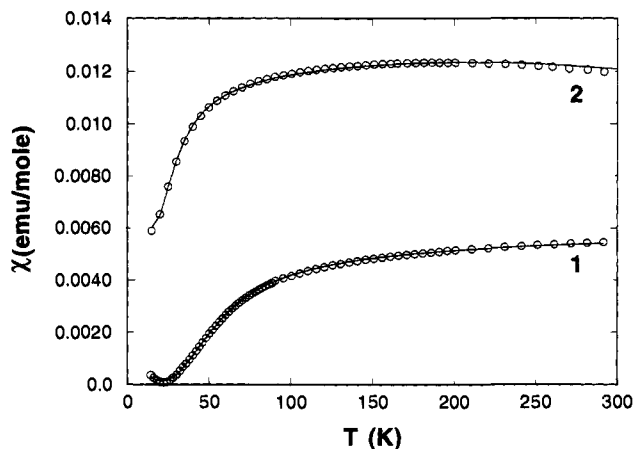


Figure 3. Magnetic susceptibility data for **1** and **2**. The dots represent experimental data. Solid lines were calculated with the expressions of ref 21 for **1** using $g = 2.0$, $J = +113$ cm⁻¹, a monomeric high-spin Fe^{III} impurity $\rho = 0.002$, and diamagnetic correction for sample holder and sample, 0 cm²/mol. Solid lines were calculated with the expressions of ref 21 for **2** using $g = 2.0$, $J = +54$ cm⁻¹, $\rho = 0.014$, and diamagnetic correction for sample holder and sample, -0.0015 cm²/mol.

For comparison, the susceptibility data for **1** are also shown in Figure 3; they are best fit with $J = +113(10)$ cm⁻¹. The J values of **1** and **2** are significantly smaller than those of all other (μ -oxo)diiron(III) complexes.¹¹ Indeed, the J value of the bis(μ -oxo) complex **2** approaches values observed for (μ -alkoxo)diiron(III) (52 cm⁻¹ for [Fe₂HPTB(O₂CC₆H₄-4-F)₂](ClO₄)₃, and

49 cm⁻¹ for [Fe₂(5,6-Me₂HPTB)(OH)(NO₃)₂](NO₃)₂) and (μ -hydroxo)diiron(III) (34 cm⁻¹ for [Fe₂(OH)(O₂CCH₃)₂(HBpz₃)₂](ClO₄) complexes.^{17,18}

(μ -Oxo)diiron(III) complexes have J values ranging from 180 to 250 cm⁻¹.¹¹ The J value is thought to reflect essentially the exchange pathway through the oxo bridge and should depend on the Fe-O bond lengths and the Fe-O-Fe angle. It has been noted that J is not very sensitive to the Fe-O-Fe angle. This insensitivity has been rationalized by Girerd *et al.*, who considered the angular dependence of the z^2-z^2 , $xz-xz$, and z^2-xz interactions for angles from 120° to 180°.¹⁹ Since **2** has two μ -oxo exchange pathways, one might have expected a substantially larger J than observed for complexes with only one oxo bridge. However, it has been noted by Gorun and Lippard that J decreases sharply (roughly exponentially) with the length of the shortest Fe-O-Fe pathway.²⁰ Thus the longer Fe-O-Fe bonds found for **1** and **2** would be expected to give rise to smaller J values. Interestingly, the J values of **1** and **2** are even smaller than predicted by the correlation of Gorun and Lippard (170 and 80 cm⁻¹ based on average Fe-O distances of 1.82 and 1.88 Å, respectively). Since **1** and **2** represent the first (μ -oxo)diiron(III) complexes with such acute Fe-O-Fe angles, it is likely that these smaller angles play a role in the weakening of the antiferromagnetic interaction.

In conclusion, we have synthesized the first bis(μ -oxo)diiron(III) complex and found it to have novel structural and magnetic properties. These provide benchmarks with which to judge the proposition that such cores may participate in the oxygen activation mechanisms of methane monooxygenase and related enzymes.

Acknowledgment. This work was supported by grants from the National Institutes of Health (GM 38767 to L.Q. and GM 22701 to E.M.). We are grateful to Professor J. D. Britton for his expertise and assistance in the X-ray diffraction experiments and a reviewer for pointing out the notion that the repulsion between the two oxo bridges may contribute to the acute Fe-O-Fe angle observed.

Supplementary Material Available: Tables of the atomic coordinates, thermal parameters, bond lengths, and bond angles for [Fe₂(O)₂(6TLA)₂](ClO₄)₂ (13 pages). This material is contained in many libraries on microfiche, immediately follows this article in the microfilm version of the journal, and can be ordered from the ACS; see any current masthead page for ordering information.

JA943386K

(15) Determination of J by Mössbauer spectroscopy is possible because the ⁵⁷Fe nucleus senses an internal magnetic field when paramagnetic excited states of the spin ladder become thermally populated. In the high-temperature limit and for fast spin relaxation, the internal field, H_{int} , for the present system is related to the molar susceptibility χ by $H_{\text{int}} = \chi H_{\text{app}} A / (2Ng\beta_n\beta)$, where A is the magnetic hyperfine coupling constant of the high-spin Fe^{III}. Using $A = -29$ MHz, a value typical for octahedral N/O coordination,¹⁶ J was determined by fitting a series of $H_{\text{app}} = 8.0$ T spectra recorded between 4.2 and 150 K to $\mathbf{H} = J\mathbf{S}_1\mathbf{S}_2 + \sum\{\mathbf{S}_i\mathbf{D}_i\mathbf{S}_i + 2\beta\mathbf{H}_{\text{app}}\mathbf{S}_i\}$, with $i = 1, 2$; for $J = 68$ cm⁻¹ and $D_1 = D_2 = 0$, this Hamiltonian gives a readily observable $H_{\text{int}} = -0.6$ T at 100 K. For $T > 50$ K and $|D_i| < 5$ cm⁻¹, the Mössbauer spectra are essentially independent of D_i .

(16) Juarez-Garcia, C.; Hendrich, M. P.; Holman, T. R.; Que, L., Jr.; Münck, E. *J. Am. Chem. Soc.* **1991**, *113*, 518-525.

(17) (a) Chen, Q.; Lynch, J. B.; Gomez-Romero, P.; Ben-Hussein, A.; Jameson, G. B.; O'Connor, C. J.; Que, L., Jr. *Inorg. Chem.* **1988**, *27*, 2673-2681. (b) Brennan, B. A.; Chen, Q.; Juarez-Garcia, C.; True, A. E.; O'Connor, C. J.; Que, L., Jr. *Inorg. Chem.* **1991**, *30*, 1937-1943.

(18) Armstrong, W. H.; Lippard, S. J. *J. Am. Chem. Soc.* **1984**, *106*, 4632-4633.

(19) Hotzelmann, R.; Wieghardt, K.; Flörke, U.; Haupt, H.-J.; Weathurburn, D. C.; Bonvoisin, J.; Blondin, G.; Girerd, J.-J. *J. Am. Chem. Soc.* **1992**, *114*, 1681-1696.

(20) Gorun, S. M.; Lippard, S. J. *Inorg. Chem.* **1991**, *30*, 1625-1630.

(21) O'Connor, C. J. *Prog. Inorg. Chem.* **1982**, *29*, 203-283.